

SEP: Self-Enhanced Prompt Tuning for Visual-Language Model

Hantao Yao¹, Rui Zhang², Lu Yu³, Changsheng Xu¹

¹ Institute of Automation, Chinese Academy of Sciences

² Institute of Computing Technology, Chinese Academy of Sciences

³ Tianjin University of Technology

hantao.yao@nlpr.ia.ac.cn

Abstract

Prompt tuning based on Context Optimization (CoOp) effectively adapts visual-language models (VLMs) to downstream tasks by inferring additional learnable prompt tokens. However, these tokens are less discriminative as they are independent of the pre-trained tokens and fail to capture input-specific knowledge, such as class-aware textual or instance-aware visual knowledge. Leveraging the discriminative and generalization capabilities inherent in pre-trained tokens, we introduce a novel approach named Self-Enhanced Prompt Tuning (SEP). The core principle of SEP involves adapting the learnable prompt tokens at each encoder layer from the corresponding self-pretrained tokens, thereby explicitly incorporating discriminative prior knowledge to enhance both textual-level and visual-level embeddings. Furthermore, SEP’s self-enhanced tokens not only boost discrimination but also mitigate domain shifts in unseen domains, enhancing generalization. In practice, SEP selects several representative tokens from all pre-trained tokens for each input data at every layer of the text/visual encoders. Subsequently, a Token Fusion Module (TFM) is introduced to generate a self-enhanced token by merging these representative tokens with the learnable tokens using a cross-attention mechanism. This self-enhanced token is then concatenated with all pre-trained tokens, serving as input for subsequent encoder layers to produce the relevant embeddings. Comprehensive evaluations across various benchmarks and tasks confirm SEP’s efficacy in prompt tuning. Code: <https://github.com/htyao89/SEP>.

1 Introduction

Recent studies demonstrate that the Visual Language Model (VLM) possesses a robust generalization capability in a variety of downstream tasks [2; 33]. However, the direct application of VLMs in scenarios with limited images is challenging because of their extensive parameters and the substantial image datasets required for training. Prompt tuning has recently emerged as an effective and straightforward method for leveraging the general knowledge of VLMs in specialized computer vision and machine learning tasks such as zero-shot learning, domain adaptation, domain generalization, and few-shot learning.

Prompt tuning combines additional learnable tokens with pre-trained ones to generate a discriminative embedding, termed Context Optimization (CoOp) [52]. Recent advances in CoOp-based methods [52; 45; 4; 31; 17; 5; 22; 18; 41; 54] aim to develop input-relevant prompt tokens to enhance the discriminative power of embeddings, as illustrated in Figure 1(a). The term ‘input-irrelevant prompt’ refers to a prompt initialized random that does not depend on specific input-related knowledge. However, since these prompts are derived from the training domain, they may exhibit domain

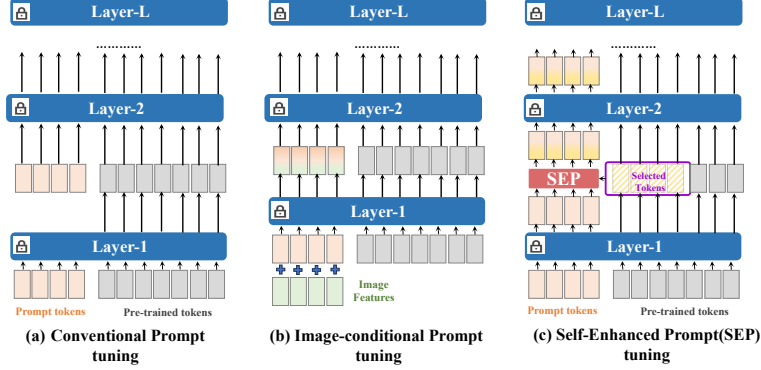


Figure 1: Comparison with existing framework. (a) Conventional input-irrelevant prompt tuning; (b) Image-conditional prompt tuning; (c) Self-enhanced prompt tuning by injecting the discriminative and generalizable knowledge contained in the frozen tokens.

shifts from unseen domains, potentially degrading performance. In addition, image-conditional prompts, which incorporate image features into the learnable tokens, have been proposed in [51; 48] (see Figure 1(b)). Despite their specificity, the image-conditional prompts have a limited ability to enhance the class-level classifier. In summary, while existing CoOp-based methods generate learnable tokens that are independent of input knowledge, they struggle to utilize essential input-aware prior knowledge, such as instance-aware visual knowledge or class-aware textual knowledge. Therefore, how to incorporate discriminative and generalizable input-aware knowledge into learnable prompts is crucial to enhancing their effectiveness for prompt tuning.

Existing methods have demonstrated that the frozen CLIP, trained with a large scale of images, possesses robust generalization capabilities for new classes or images. For example, CLIP exhibits remarkable performance in zero-shot learning and domain generalization, indicating that frozen tokens corresponding to each input contain essential generalizable knowledge. In addition, these frozen tokens can be used to improve the discriminative and generalization of learnable prompts, resulting in prompts that contain the prior discriminative knowledge related to each input. To better mine more useful knowledge, several representative tokens are selected from the pool of all frozen tokens. These representative tokens are then integrated with the tokens corresponding to the learnable prompt to generate the input-aware prompt. This integration leverages the knowledge embedded in the frozen tokens, endowing the resultant input-aware tokens with several advantages. Unlike the input-irrelevant prompt, input-aware prompts are related to each input due to their incorporation of specific knowledge from the frozen token, thereby enhancing their generalizability. Furthermore, discriminative knowledge within the representative tokens injects the input-aware prompt with discriminative capabilities. In summary, by associating pre-trained tokens with learnable prompts, a robust input-aware token is generated, significantly boosting both the generalization and discriminative capacities of prompt tuning.

In this work, we propose a novel approach named Self-Enhanced Prompt Tuning (SEP), as depicted in Figure 2. SEP introduces a Token-Fusion Module (TFM) to incorporate the essential knowledge from pre-trained tokens into input-aware tokens. Specifically, TFM selects a subset of highly discriminative pre-trained tokens for each input from the middle layers. It then employs a multi-head attention mechanism to integrate these selected tokens with the corresponding prompt-related tokens for generating a self-enhanced prompt token. Subsequently, the enhanced token is concatenated with the pre-trained tokens and processed by subsequent encoder layers. In particular, TFM can be seamlessly integrated into the middle layers of both visual and textual encoders in the CLIP.

The proposed Self-Enhanced Prompt Tuning (SEP) significantly improves discriminativeness and generalizability for downstream tasks by injecting the essential knowledge contained in the pre-trained tokens. The effectiveness of SEP is validated in several tasks and benchmarks: base-to-new settings, domain generalization, cross-dataset generalization, and few-shot learning. The major contributions of SEP include: 1) the introduction of an innovative Self-Enhanced Prompt tuning mechanism, which integrates self-enhanced prompt tokens generated by the Token-Fusion Module (TFM) into visual/textual encoders; 2) we claim that the injection of prior discriminative knowledge

from pre-trained tokens into learnable prompt tokens can enhance the discriminative and generalizable of the generated embeddings.

2 Related Works

Vision-Language Models: Recently, Vision-Language Models (VLMs) [33; 2], which utilize both visual and textual encoders, have been trained on a large-scale dataset of image-text pairs, demonstrating significant generalization and discrimination capabilities. To further enhance the descriptive power of VLMs, improvements have been made in several areas: (1) employing more robust text or visual encoders [42; 49; 25]; (2) integrating visual and textual knowledge more deeply [24; 39]; and (3) increasing the volume of images used [33; 16; 36; 37]. To enhance the diversity of text descriptions, Masked Language Modeling (MLM) [20; 27] has been employed, which randomly omits words in the text to aid in representation learning. In contrast to MLM, masked autoencoder-based methods [13] have been introduced to improve descriptive capabilities by randomly masking image patches. Among the VLM frameworks, CLIP stands out as a straightforward yet effective model that uses contrastive loss to train separate visual and text encoders based on 400 million image-text pairs. Given its robust generalization, many CoOp-based methods have been developed using CLIP to adapt pre-trained VLMs for downstream tasks. In this work, we have implemented a prompt-tuning strategy to generate task-specific embeddings.

Prompt Tuning: To adapt pre-trained Vision-Language Models (VLMs) to downstream tasks, various strategies involving prompt tuning have been employed [10; 31; 22; 48; 33; 23]. Initially, CLIP[33] uses a hand-crafted template ‘a photo of a [CLASS]’ for zero-shot prediction. However, these hand-crafted prompts often fail to adequately capture the nuances of downstream tasks, leading to the development of textual prompt tuning strategies that use learnable textual tokens alongside class tokens to enhance textual embeddings. For example, the hand-crafted prompts are replaced with the learnable prompt tokens in Context Optimization(CoOp) [52]. Moreover, Conditional Context Optimization(CoCoOp) [51] and VPT [48] generate an image-conditional prompt fusing the image feature and the learnable textual prompt to boost generalization in the unseen domain. To better use the essential knowledge contained in frozen CLIP, Knowledge-Guided Context Optimization(KgCoOp) [45], ProGrad [53], and Prompt Regularization(ProReg) [54] all construct a novel constraint term by constraining the consistency between the learnable knowledge and the essential general knowledge. Unlike the above methods, which consider textual prompts, Ensembling Context Optimization(ECO) [1] employs prompt ensembling to combine multiple prompts. Furthermore, ProDA [28] considers the prompt’s prior distribution learning, and Distribution-Aware Prompt Tuning (DAPT) [5] optimizes the learnable prompt by maximizing inter-dispersion. Knowledge-Aware Prompt Tuning(KAPT) [17] employs external knowledge to boost generalization on unseen classes. PLOT [4] applies optimal transport to match the vision and text modalities for generating the discriminative and visual-aligned local textual prompt tokens. Besides the textual prompt tuning, Multi-modal Prompt Learning (MaPLe) [18] and PromptSRC [19] conduct the visual-textual prompt tuning by jointly conducting the prompt tuning on the visual and text encoders. Multitask Vision-Language Prompt Tuning (MVLPT) [38] integrates cross-task knowledge, enhancing the versatility of prompt tuning in VLMs. Finally, DenseCLIP [34] and CLIP-Adapter [12] introduce context-aware strategies and adapters to refine the embeddings for specific tasks, further illustrating the dynamic evolution of prompt tuning in the field of vision-language models. Recently, GraphAdaper [26] is proposed to fuse visual and textual knowledge with two Graph-based Adapters, and the Class-aware prompt is proposed in TCP [46] to inject class-level knowledge into the prompt.

Existing methods generate two types of input-irrelevant and image-conditional tokens, exhibiting limited capability to capture specific knowledge. To address this issue, we introduce a novel Self-Enhanced Prompt Tuning, which utilizes the Token Fusion Module (TFM) to integrate discriminative knowledge from self-pretrained tokens into the enhanced prompts, thereby enriching the prompt’s contextual relevance. Unlike traditional CoOp-based methods, our technique distinctively generates prompt tokens by leveraging these self-pretrained tokens. Our evaluations across various tasks and benchmarks demonstrate that this integration significantly boosts the discriminative power of the prompt tuning process, confirming the efficacy of the proposed SEP.

3 Methodolgy

3.1 Preliminaries

The frozen Contrastive Language-Image Pre-training (CLIP) trained with a large number of images exhibits robust generalization capacity to new classes or images, *e.g.*, CLIP shows impressive performance on zero-shot learning and domain generalization tasks. Therefore, existing prompt tuning based on Context Optimization (CoOp) is proposed based on CLIP. Given an image along with all class names, CLIP extracts the visual and text embeddings with the visual and text encoders, and the contrast loss is calculated to align those two embeddings. To effectively adapt CLIP for the downstream task, CLIP applies the hand-crafted template "a photo of a {" to extract the general class-level textual embedding, defined as $\mathbf{W}^{clip} = \{\mathbf{w}_i^{clip}\}_{i=1}^{N_c}$, where \mathbf{w}_i^{clip} is the textual embedding of i -th class, and N_c is the number of classes. Given the 'class-name' of i -th class, Word Embedded $e(\cdot)$ first embeds the hand-crafted description into a vectorized textual tokens: $\mathbf{t}_i^{clip} = e(\text{"a photo of a {class-name}"})$. After that, Text Encoder ψ maps the vectorized textual tokens \mathbf{t}_i^{clip} to the class-level embedding: $\mathbf{w}_i^{clip} = \psi(\mathbf{t}_i^{clip})$.

In addition, Context Optimization (CoOp) replaces hand-crafted text tokens with learnable text tokens $\mathbb{T} = \{\mathbf{t}_1, \mathbf{t}_2, \dots, \mathbf{t}_M\}$, where M is the length of the tokens. Similarly to CLIP, the corresponding class token \mathbf{c}_i is concatenated with the learnable tokens \mathbb{T} to generate the textual token $\mathbf{t}_i^{coop} = \{\mathbf{t}_1, \mathbf{t}_2, \dots, \mathbf{t}_M, \mathbf{c}_i\}$. Next, textual embedding \mathbf{w}_i^{coop} is obtained by feeding textual tokens \mathbf{t}_i^{coop} into the Text Encoder ψ , *i.e.*, $\mathbf{w}_i^{coop} = \psi(\mathbf{t}_i^{coop})$. Finally, textual embeddings of all classes are defined as $\mathbf{W}^{coop} = \{\mathbf{w}_i^{coop}\}_{i=1}^{N_c}$. CoOp infers the learnable textual tokens \mathbb{T} by minimizing the contrastive loss between the image's embedding \mathbf{f} and its class embedding \mathbf{w}_y^{coop} :

$$\mathcal{L}_{ce} = \frac{1}{N} \sum_{(\mathbf{f}, y) \in \mathcal{D}_s} \frac{\exp(d(\mathbf{f}, \mathbf{w}_y^{coop})/\tau)}{\sum_{i=1}^{N_c} \exp(d(\mathbf{f}, \mathbf{w}_i^{coop})/\tau)}, \quad (1)$$

where \mathcal{D}_s is the seen dataset, and $d(\cdot)$ is the cosine distance. τ is a temperature factor defined in CLIP, and N is the number of training images.

As the generated textual embedding has a good generalization ability for the novel classes, KgCoOp further adds an efficient consistency \mathcal{L}_{kg} between the generated embedding \mathbf{W}^{coop} and the general embedding \mathbf{W}^{clip} ,

$$\mathcal{L}_{kg} = \|\mathbf{W}^{clip} - \mathbf{W}^{coop}\|_2^2. \quad (2)$$

Therefore, a robust objective for prompt tuning is:

$$\mathcal{L} = \mathcal{L}_{ce} + \omega \mathcal{L}_{kg}, \quad (3)$$

where ω is set as 8.0 same as in KgCoOp [45].

3.2 Self-Enhanced Prompt Tuning

Most existing CoOp-based methods infer input-irrelevant and image-conditional prompt tokens for prompt tuning. However, the input-irrelevant prompts are typically derived from the seen domain, inherently biasing them from the unseen domain and consequently degrading performance. Additionally, image-conditional prompt tokens that incorporate image-specific knowledge are less effective in mitigating domain shifts at the class level. A significant limitation of current approaches is their inability to encapsulate prior essential knowledge; for instance, neither visual nor textual prompts adequately capture instance-aware visual knowledge or class-aware textual knowledge within the visual or text encoders, respectively. Recognizing that essential knowledge generated by the frozen CLIP model exhibits high discriminative and generative capabilities, a reasonable motivation is to leverage this inherent knowledge to boost the prompt tuning. By integrating essential knowledge from frozen tokens into learnable prompts, an enhanced token that is aware of the input can be generated that offers distinct advantages. Firstly, input-aware prompt tokens inherit discriminative knowledge from frozen tokens, enhancing the discriminative capacity of generated embeddings across both seen and unseen domains. Secondly, these tokens possess enhanced generability for unseen domains because the frozen tokens from these domains provide crucial insights that guide the embedding generation during testing. In summary, by fusing frozen tokens with learnable prompts, we can

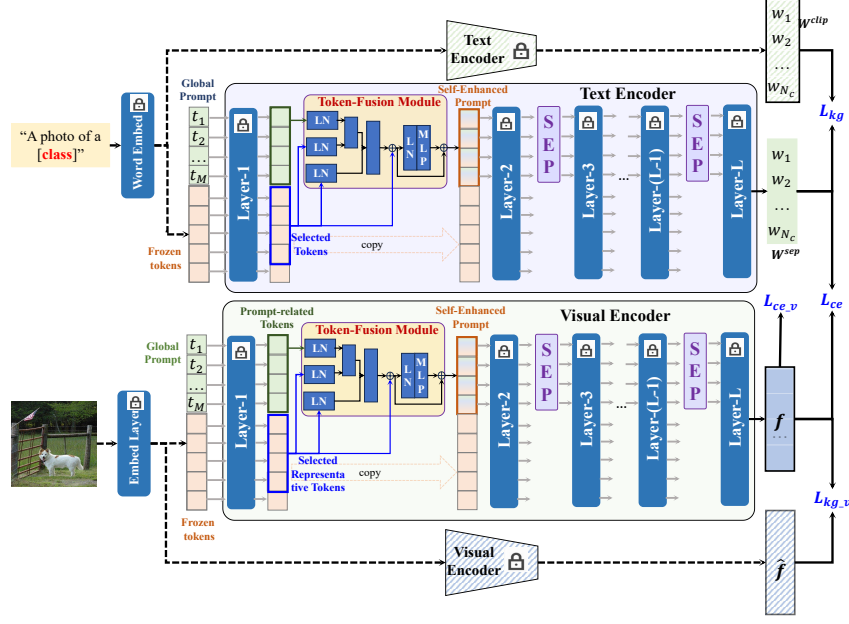


Figure 2: The framework of the proposed Self-Enhanced Prompt tuning. The Token-Fusion Module is used to integrate the pre-trained tokens and the prompt-related tokens for generating the self-enhanced prompt.

formulate robust input-aware tokens that significantly boost the generalization and discriminative capabilities of prompt tuning. Therefore, we introduce a novel Self-Enhanced Prompt Tuning (SEP), as depicted in Figure 2. Notably, SEP can be easily applied to both Visual and Text Encoders, and we introduce the application of SEP on the Visual Encoder as an illustrative example.

Given the batch images \mathbf{X} consisting of N_b images, we first apply the pre-trained Embedding Layer $\mathcal{E}(\cdot)$ to extract the frozen image tokens $\mathbf{E} \in \mathbb{R}^{L_e \times N_b \times D_v}$, where $L_e = 193$ and $D_v = 768$ are tokens' length and dimension for CLIP with ViT-B/16. Similarly to multi-modal prompt tuning [18], a global visual prompt $\mathbf{P}_g \in \mathbb{R}^{L_v \times D_v}$ is first combined with the frozen image tokens \mathbf{E} , where L_v is the length of the global visual prompt. Basically, the extended image tokens are $\mathbf{V}_0 = [\mathbf{E}, \mathbf{P}_g] \in \mathbb{R}^{(L_e + L_v) \times N_b \times D_v}$. Subsequently, the extended image tokens \mathbf{V}_0 are fed into the Visual Encoder θ for embedding. Specifically, the first layer of the Visual Encoder θ_1 projects the image tokens \mathbf{V}_0 into the middle token \mathbf{V}_1 ,

$$\mathbf{V}_1 = \theta_1(\mathbf{V}_0), \mathbf{V}_0 = [\mathbf{E}, \mathbf{P}_g]. \quad (4)$$

Self-Enhanced Prompt tuning: Once the token \mathbf{V}_1 is obtained, Self-Enhanced Prompt(SEP) tuning is proposed to generate the corresponding self-enhanced tokens $\hat{\mathbf{V}}_1$ with Token-Fusion Module(TFM). Note that the image token $\mathbf{V}_1 = [\mathbf{V}_1^v, \mathbf{V}_1^p]$ can be split into two components: the pre-trained visual tokens $\mathbf{V}_1^v = \mathbf{V}_1[1 : L_e, :, :]$, and the prompt-related tokens $\mathbf{V}_1^p = \mathbf{V}_1[L_e + 1 : L_e + L_v, :, :]$ ¹. The pretrained visual tokens \mathbf{V}_1^v are mostly related to the pre-trained image tokens \mathbf{E} that contain the essential discriminative and generalization knowledge, while the prompt-related tokens are most related to the additional learnable prompt to capture the transfer knowledge.

Unlike existing methods that simply fed the prompt-related tokens \mathbf{V}_1^p into the next layer, Token-Fusion Module(TFM) (\mathcal{T}^v) is proposed to generate the self-enhanced token $\hat{\mathbf{V}}_1^p$ by associating the pre-trained visual tokens \mathbf{V}_1^v and the prompt-related tokens \mathbf{V}_1^p ,

$$\hat{\mathbf{V}}_1^p = \mathcal{T}^v(\mathbf{V}_1^v, \mathbf{V}_1^p). \quad (5)$$

The generated self-enhanced token $\hat{\mathbf{V}}_1^p$ has inherited the essential knowledge from the pre-trained visual tokens \mathbf{V}_1^v , which means that the generated embedding has enough discriminative ability. After

¹For the visual prompt tuning, the prompt-related tokens are always inserted after the original visual tokens.

that, the self-enhanced token $\hat{\mathbf{V}}_1^p$ is combined with the pre-trained visual tokens \mathbf{V}_1^v to generate the new visual tokens $\hat{\mathbf{V}}_1 = [\mathbf{V}_1^v, \hat{\mathbf{V}}_1^p]$, fed into the next layers for embedding.

Overall, given the current token \mathbf{V}_l of l -th layer ($l \geq 1$), SEP with the Token-Fusion Module (\mathcal{T}^v) can be formulated as follows,

$$\mathbf{V}_{l+1} = \theta_{l+1}([\mathbf{V}_l^v, \mathcal{T}_l^v(\mathbf{V}_l^v, \mathbf{V}_1^p)]), (l \geq 1), \quad (6)$$

where θ_{l+1} is the $(l+1)$ -th layer in Visual Encoder.

Token-Fusion Module: In Eq. (6), Token-Fusion Module (\mathcal{T}^v) is the critical aspect for the proposed SEP. We next give a detailed description of the Token-Fusion Module (TFM). Given the pre-trained visual tokens $\mathbf{V}_l^v \in \mathbb{R}^{L_e \times N_b \times D_v}$, TFM first selects L_v representative tokens $\hat{\mathbf{V}}_l^v$ from all L_e visual tokens, leading to the same dimension as the prompt-related tokens \mathbf{V}_1^p . Moreover, the activation score of a feature can represent its discriminative ability, *i.e.*, the element with a higher activation score represents the more discriminative. Therefore, we choose the top- L_v tokens with the highest activation score. Note that the activation score of each token is the average of the feature's value after the square. Consequently, we can obtain top- L_v tokens $\hat{\mathbf{V}}_l^v$. After that, cross-attention is applied to fuse the selected visual tokens $\hat{\mathbf{V}}_l^v$ and the prompt-related tokens \mathbf{V}_1^p ,

$$\hat{\mathbf{V}}_l^p = \mathcal{T}_l^v(\hat{\mathbf{V}}_l^v, \mathbf{V}_1^p) \quad (7)$$

$$= \text{softmax} \left(\frac{\hat{\mathbf{V}}_l^v (\mathbf{V}_1^p)^\top}{\sqrt{d_k}} \right) \hat{\mathbf{V}}_l^v, \quad (8)$$

where $\hat{\mathbf{V}}_l^p$ is the generated self-enhanced token, and d_k is the dimension of keys. $\hat{\mathbf{V}}_l^p$ is concated with the frozen visual tokens \mathbf{V}_l^v to generate the new visual tokens $\hat{\mathbf{V}}_1 = [\mathbf{V}_1^v, \hat{\mathbf{V}}_1^p]$, fed into the next layers for embedding.

Importantly, the proposed SEP can also be easily applied to the Text Encoder for textual prompt tuning. When performing SEP on the Text Encoder, the representative tokens are selected by the front top- L_t tokens containing the discriminative knowledge based on the hand-crafted templates "a photo of a {class-name}".

Objective: Given the image x , labels, and the class names, we first use the frozen CLIP to extract the frozen text-level classifier \mathbf{W}^{clip} and the visual embedding \mathbf{f} . By performing the proposed SEP on the Visual Encoder and the Textual Encoder, we can generate the enhanced text-level classifier \mathbf{W}^{sep} and the enhanced visual embedding $\hat{\mathbf{f}}$. To increase the discrimination of the enhanced visual embedding, a cross-entropy loss \mathcal{L}_{ce_v} is conducted on the visual embedding $\hat{\mathbf{f}}$. Inspired by KgCoOp [45], we also conduct the consistency constraint \mathcal{L}_{kg_v} between the original visual embedding \mathbf{f} and the enhanced visual embedding $\hat{\mathbf{f}}$:

$$\mathcal{L}_{kg_v} = \|\hat{\mathbf{f}} - \mathbf{f}\|_2^2. \quad (9)$$

By considering Eq. (3), the final objective is:

$$\mathcal{L} = \mathcal{L}_{ce}(\hat{\mathbf{f}}, \mathbf{W}^{sep}) + \omega_t \mathcal{L}_{kg}(\mathbf{W}^{clip}, \mathbf{W}^{sep}) + \omega_v \mathcal{L}_{kg_v}(\hat{\mathbf{f}}, \mathbf{f}) + \mathcal{L}_{ce_v}(\hat{\mathbf{f}}), \quad (10)$$

where ω_t and ω_v are the weight to balance the effect of the consistency of the textual-level embedding and visual embeddings. Similarly to KgCoOp [45], ω_t is set as 8.0. The effect of ω_v is given in the experiment.

4 Experiments

4.1 Experimental Setup

Dataset. We conduct the evaluation on the following benchmarks, *i.e.*, ImageNet [7], Caltech [9], OxfordPets [32], StanfordCars [21], Flowers [30], Food101 [3], FGVC Aircraft [29], EuroSAT [14], UCF101 [40], DTD [6], and SUN397 [44]. Moreover, we use the ImageNet and its variants for domain generalization, *i.e.*, the ImageNet is treated as the source domain; ImageNetV2 [35], ImageNet-Sketch [43], ImageNet-A [11] and ImageNet-R [15] are treated as the target domains for evaluation.

Table 1: Comparion on the base-to-new generalization. ‘*’ denotes the results are based our re-implemented.

	Sets	CoOp*	CoCoOp	DAPT*	ProGrad*	ProDA	KgCoOp	RPO	PLOT*	LFA	MaPLe	DePT	PromptSRC	TCP	SEP
Average	Base	82.38	80.47	83.18	82.48	81.56	80.73	81.13	83.98	83.62	82.28	83.62	84.26	84.13	85.98
	New	67.96	71.69	69.27	70.75	72.30	73.6	75.00	71.72	74.56	75.14	75.04	76.10	75.36	76.49
	H	74.48	75.83	75.59	76.16	76.65	77.0	77.78	77.37	78.83	78.55	79.10	79.97	79.51	80.96
ImageNet	Base	76.46	75.98	76.83	77.02	75.40	75.83	76.60	77.30	76.89	76.66	77.03	77.60	77.27	78.10
	New	66.31	70.43	69.27	66.66	70.23	69.96	71.57	69.87	69.36	70.54	70.13	70.73	69.87	69.55
	H	71.02	73.10	72.85	71.46	72.72	72.78	74.00	73.40	72.93	73.47	73.42	74.01	73.38	73.58
Caltech	Base	97.80	97.96	97.83	98.02	98.27	97.72	97.97	98.53	98.41	97.74	98.30	98.10	98.23	98.80
	New	93.27	93.81	93.07	93.89	93.23	94.39	94.37	92.80	93.93	94.36	94.60	94.03	94.67	94.53
	H	95.48	95.84	95.39	95.91	95.68	96.03	96.03	95.58	96.13	96.02	96.41	96.02	96.42	96.62
Pets	Base	94.47	95.20	95.00	95.07	95.43	94.65	94.63	94.50	95.13	95.43	94.33	95.33	94.67	95.37
	New	96.00	97.69	95.83	97.63	97.83	97.76	97.50	96.83	96.23	97.76	97.23	97.30	97.20	97.40
	H	95.23	96.43	95.41	96.33	96.62	96.18	96.05	95.65	95.68	96.58	95.76	96.30	95.92	96.37
Cars	Base	75.67	70.49	75.80	77.68	74.70	71.76	73.87	79.07	76.32	72.94	79.13	78.27	80.80	83.77
	New	67.53	73.59	63.93	68.63	71.20	75.04	75.53	74.80	74.88	74.00	75.47	74.97	74.13	75.43
	H	71.37	72.01	69.36	72.88	72.91	73.36	74.69	76.88	75.59	73.47	77.26	76.58	77.32	79.38
Flowers	Base	97.27	94.87	96.97	95.54	97.70	95.00	94.13	97.93	97.34	95.92	98.00	98.07	97.73	98.17
	New	67.13	71.75	60.90	71.87	68.68	74.73	76.60	73.53	75.44	72.46	76.37	76.50	75.57	76.63
	H	79.44	81.71	74.81	82.03	80.66	83.65	84.50	83.99	85.00	82.56	85.84	85.95	85.23	86.07
Food	Base	89.37	90.70	90.37	90.37	90.30	90.5	90.33	89.80	90.52	90.71	90.50	90.67	90.57	90.60
	New	88.77	91.29	91.30	89.59	88.57	91.7	90.83	91.37	91.48	92.05	91.60	91.53	91.37	91.60
	H	89.07	90.99	90.83	89.98	89.43	91.09	90.58	90.58	91.00	91.38	91.05	91.10	90.97	91.10
Aircraft	Base	39.67	33.41	39.97	40.54	36.90	36.21	37.33	42.13	41.48	37.44	43.20	42.73	41.97	49.17
	New	31.23	23.71	29.80	27.57	34.13	33.55	34.20	33.73	32.29	35.61	34.83	37.87	34.43	35.17
	H	34.95	27.74	34.14	32.82	35.46	34.83	35.70	37.46	36.31	36.50	38.57	40.15	37.83	41.01
SUN397	Base	80.85	79.74	80.97	81.26	78.67	80.29	80.60	82.20	82.13	80.82	82.33	82.67	82.63	82.77
	New	68.34	76.86	76.97	74.17	76.93	76.53	77.80	73.63	77.20	78.70	77.80	78.47	78.20	78.80
	H	74.07	78.27	78.92	77.55	77.79	78.36	79.18	77.68	79.59	79.75	80.00	80.52	80.35	80.74
DTD	Base	79.97	77.01	82.23	77.35	80.67	77.55	76.70	81.97	81.29	80.36	82.20	82.37	82.77	85.5
	New	48.60	56.00	54.23	52.35	56.48	54.99	62.13	43.80	60.63	59.18	59.13	62.97	58.07	61.97
	H	60.46	64.85	65.36	62.45	66.44	64.35	68.61	57.09	69.46	68.16	68.78	71.75	68.25	71.86
EuroSAT	Base	90.10	87.49	94.73	90.11	83.90	85.64	86.63	93.70	93.40	94.07	89.03	92.90	91.63	95.3
	New	53.00	60.04	50.33	60.89	66.00	64.34	68.97	62.67	71.24	73.23	71.07	73.90	74.73	79.6
	H	66.74	71.21	65.74	72.67	73.88	73.48	76.79	75.11	80.83	82.3	79.04	82.32	82.32	86.75
UCF101	Base	84.53	82.33	84.30	84.33	85.23	82.89	83.67	86.60	86.97	83.00	85.80	87.10	87.13	88.23
	New	67.37	73.45	76.33	74.94	71.97	76.67	75.43	75.90	77.48	78.66	77.23	78.80	80.77	80.73
	H	74.98	77.67	80.12	79.35	78.04	79.65	79.34	80.90	81.95	80.77	81.29	82.74	83.83	84.31

Training Details. Our implementation is adapted from the public code [52; 45] based on the CLIP with the backbone of ViT-B/16 [8]. The prompt’s length L_v and L_t is set as 4 and 6 for the visual prompt tuning and textual prompt tuning. The hand-crafted templates initialized with "X X X X X X { }" are used for the textual prompt tuning. The final performance is averaged over three standard random seeds(1/2/3). Adam optimizer is applied for optimization with the learning rate of 2.5e-3 and the batch size of 32 up to the training epochs is 50. All experiments are conducted on RTX 3090.

Baselines. Recently CoOp-based methods are used for comparison, *e.g.*, CoOp [52], CoCoOp [51], ProGrad [53], ProDA [28], KgCoOp [45], PromptSRC [19], MaPLe [18], LFA [31], DePT [50], DAPT [5], PLOT [4], TaskRes [47], RPO [22], VPT [48], GraphAdaper [26], and TCP [46].

4.2 Comparison with Existing methods

In this section, we compare the proposed SEP with the existing methods from four types of tasks.

Base-to-New Class Generalization: Similar to existing CoOp-based methods, a significant evaluation of prompt tuning is the base-to-new generalization setting consisting of two disjoint subsets: *Base* and *New* classes. The base-to-new generalization can be treated as zero-shot learning, which infers the trainable parameter with the labeled *Base* classes and is evaluated on the disjointed *New* classes. As shown in Table 1, the proposed SEP obtains the highest average performance in the term of Base/New/H, *e.g.*, obtaining the Base/New/H of 85.98%/76.49%/80.96%. Since SEP can effectively inject the prior discriminative knowledge inheriting from the pre-trained visual tokens, it obtains the performance on *Base* classes of 85.98%, obtaining 1.72% improvement upon existing SOTA PromptSRC. The superior performance also demonstrates the necessity and the reasonable of considering the prior knowledge for improving the discriminative on the seen domain. Moreover, we can observe that the proposed SEP obtains the *New* performance of 76.49%, demonstrating that the use of the self-enhanced prompt can improve the generalization in the unseen domain. In conclusion,

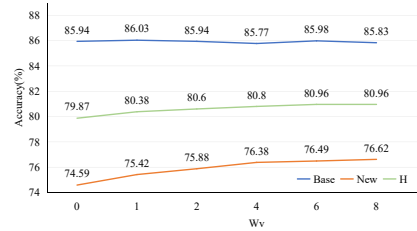
Table 2: Comparison of cross-dataset evaluation from the ImageNet to the rest Ten datasets.

Datasets	CLIP	CoOp	ProGrad	KgCoOp	DePT	VPT	PLOT	PromptSRC	MaPLe	DAPT	TCP	SEP
ImageNet	66.70	71.51	72.24	70.66	72.77	69.73	71.60	71.27	70.72	71.60	71.40	70.33
Caltech101	93.30	93.70	91.52	93.92	94.23	93.67	92.07	93.60	93.53	93.50	93.97	94.17
Pets	89.10	89.14	89.64	89.83	90.03	89.27	90.10	90.25	90.49	90.67	91.25	90.77
Cars	65.70	64.51	62.39	65.41	65.57	65.5	65.70	65.70	65.57	65.93	64.69	65.90
Flowers	70.70	68.71	67.87	70.01	70.57	70.2	69.23	70.25	72.20	71.70	71.21	71.93
Food101	85.90	85.30	85.40	86.36	86.37	86.27	86.23	86.15	86.20	86.10	86.69	86.15
Aircraft	24.90	18.47	20.16	22.51	23.27	22.13	25.00	23.90	24.74	23.03	23.45	24.77
SUN397	62.60	64.15	62.47	66.16	66.67	66.57	61.67	67.10	67.01	67.00	67.15	67.07
DTD	44.30	41.92	39.42	46.35	45.97	46.93	38.60	46.87	46.49	44.00	44.35	45.63
EuroSAT	48.30	46.39	43.46	46.04	43.53	47.43	47.83	45.50	48.06	52.47	51.45	50.97
UCF101	67.60	66.55	64.29	68.50	69.30	67.20	67.00	68.75	68.69	68.73	68.73	68.50
Avg.	65.24	63.88	62.71	65.51	65.55	65.52	64.34	65.81	66.30	66.31	66.29	66.59

Table 3: Comparison of domain generalization from ImageNet to its variants.

	ImageNet	-V2	-S	-A	-R	Avg.
CoCoOp	71.02	64.07	48.75	50.63	76.18	59.91
ProGrad	72.24	64.73	47.61	49.39	74.58	59.08
KgCoOp	71.2	64.1	48.97	50.69	76.7	60.12
MaPLe	70.72	64.07	49.15	50.9	76.98	60.27
DAPT	71.67	64.5	49.53	51.1	76.33	60.37
SEP	71.03	64.30	49.75	50.70	77.43	60.54

Figure 3: Effect of ω_v .



the superior performance of SEP shows that using the self-enhanced prompt with considering the self-pretrained tokens can boost discriminative and generalization embeddings.

Cross-Dataset Generalization: Different from the base-to-new generalization assuming that the testing dataset and training dataset have a similar data distribution with disjoint classes, the cross-dataset generalization performs the training on the base dataset (ImageNet) and evaluation on the rest ten datasets. The comparison between SEP and the existing methods is summarized in Table 2. We can observe that the proposed SEP obtains the highest average performance, *e.g.*, obtaining the average performance of 66.59%. The superior performance demonstrates the effectiveness of SEP in generating the generalization description by injecting the self-pretrained token knowledge.

Domain Generalization: Domain generalization is conducted between the imagenet and the variant of imagenets (ImageNetV2, ImageNet-Sketch, ImageNet-A, and ImageNet-R) to verify the generalization ability of the prompt tuning. The comparison with existing methods is summarized in Table 3. It can be seen that the proposed SEP obtains the best average performance of 60.54%, proving the generalizability of the proposed SEP.

Few-Shot Learning: To further verify the effectiveness of the proposed SEP, we conduct the few-shot learning with K-shot labeled images. As shown in Table 4, the proposed SEP obtains an obvious improvement over existing methods. For example, SEP obtains the average performance of 78.28%, obtaining an improvement of 1.38% over the existing PLOT. Moreover, SEP obtains the highest performance in most datasets, *e.g.*, 8/11 datasets. The reason is that the self-enhanced prompt after injecting the prior discriminative knowledge of the pre-trained tokens can provide significant clues. Especially for the few-show learning that can provide less useful knowledge, more critical knowledge can be provided by the self-enhanced prompt for inferring discriminative knowledge.

4.3 Ablation Study

We conduct several ablation studies to verify the effectiveness of SEP.

Effect of Self-enhanced Prompt tuning: To verify the effectiveness of Self-enhanced Prompt tuning(SEP), we replace SEP with the Individual Visual-Language Prompting (IVLP) [18] that conducts the individual input-independent prompt tuning. As shown in Table 5, based on the baseline

Table 4: Comparison of few-shot learning with 4-shot samples.

	CLIP	CoOp	CoCoOp	ProGrad	KgCoOp	MaPLe	TIP-Adapter	DAPT	PromptSRC	PLOT	TaskRes	TCP	SEP
ImageNet	66.70	69.37	70.55	70.21	70.19	70.67	70.78	70.80	70.80	70.40	62.87	70.48	69.93
Caltech101	93.30	94.44	94.98	94.93	94.65	94.30	94.77	94.23	94.77	95.13	94.67	95.00	95.40
Pets	89.10	91.30	93.01	93.21	93.20	92.05	92.26	92.17	93.23	92.55	92.00	91.90	92.90
Cars	65.70	72.73	69.10	71.75	71.98	68.70	74.42	74.40	71.83	76.25	75.90	76.30	77.73
Flowers	70.70	91.14	82.56	89.98	90.69	80.80	92.98	92.37	91.31	92.93	91.50	94.40	94.63
Food101	85.90	82.58	86.64	85.77	86.59	86.90	86.18	83.60	86.06	86.46	86.03	85.3	85.77
Aircraft	24.90	33.18	30.87	32.93	32.47	29.03	35.49	32.47	32.80	35.29	33.80	36.20	38.07
SUN397	62.60	70.13	70.50	71.17	71.79	71.47	70.65	72.20	72.80	71.73	72.70	72.11	73.30
DTD	44.30	58.57	54.79	57.72	58.31	54.73	61.70	61.37	60.64	62.43	59.57	63.97	66.23
EuroSAT	48.30	68.62	63.83	70.84	71.06	54.87	78.27	72.73	75.02	83.21	72.87	77.43	85.20
UCF101	67.60	77.41	74.99	77.82	78.40	73.70	79.73	79.40	79.35	79.76	76.10	80.83	81.90
Avg.	65.37	73.59	71.98	74.21	74.48	70.66	76.11	75.07	75.33	76.9	74.36	76.72	78.28

Table 5: Effect of Self-enhanced Prompt tuning.

Visual Encoder	Text Encoder	Base	New	H
IVLP	IVLP	85.91	74.99	80.08
IVLP	SEP	86.19	75.35	80.41
SEP	IVLP	85.53	74.80	79.80
SEP	SEP	85.98	76.49	80.96

Table 6: Effect of Multi-modal Prompt tuning.

Visual Encoder	Text Encoder	Base	New	H
-	-	82.86	74.30	78.35
-	SEP	84.66	75.51	79.82
SEP	-	82.94	75.17	78.86
SEP	SEP	85.98	76.49	80.96

with conducting IVLP on visual prompt tuning, using the SEP for textual prompt tuning obtains a higher performance on all three types of measure metrics, *e.g.*, improves the Base/New/H from 85.91%/74.99%/80.08% to 86.19%/75.35%/80.41%. Moreover, conducting SEP on both visual and textual prompt tuning achieves the performance of 76.49%/80.96% for New/H, obtaining 1.5%/0.9% improvement upon the ones using IVLP on both modals. The superior performance demonstrates the effectiveness of the proposed self-enhanced prompt tuning.

Effect of Multi-modal prompt tuning: SEP can be easily applied for visual prompt tuning and textual prompt tuning for Visual and Text Encoders. We thus analyze the effect of the multi-modal prompt tuning and summarize the results in Table 6. It can be observed that conducting SEP on two modals obtains a higher performance than merely one modal, proving that the two modal prompt tuning are complementary and conducting the multi-modal prompt tuning is more effective.

Effect of ω_v : The effect of the hyperparameter ω_v in the final objective(Eq. (10)) is shown in Figure 3. It can be observed that firstly increasing the hyperparameter would increase the performance while degrading the performance. Consequently, setting $\omega_v=6.0$ obtains the best performance.

Effect of Token Selective Strategy: There are two types of strategy to choose representative tokens from all pre-trained tokens: front-based and activation-based selective strategies, where the front-based strategy selects the front of L_v tokens, and the activation-based strategy selects the tokens with top- L_v high activation scores. As shown in Table 7, the front-based strategy is suitable for textual prompt tuning, and the activation-based strategy is suitable for visual prompt tuning.

Table 7: Effect of Token Selective Strategy.

Visual Encoder	Text Encoder	Base	New	H
Activation	Front	85.96	76.53	80.97
Front	Front	85.8	76.5	80.88
Front	Activation	85.31	75.84	80.30
Activation	Activation	85.38	75.70	80.25

Effect of Token Fusion Strategy: After selecting the representative tokens from all tokens, Token Fusion Module(TFM) applies the cross-attention to fuse the selected tokens and the prompt-related tokens. We further make comparison with other two token fusion strategy: Add and MLP strategies, where ‘Add’ is the add operation, and ‘MLP’ denotes use multiple fully-connected layers to fuse. As shown in Table 8, TFM with cross-attention obtains the best performance.

Table 8: Effect of Token Fusion Strategy.

Fusion Strategies	Base	New	H
Add	83.39	74.09	78.46
MLP	85.78	75.77	80.46
TFM	85.96	76.53	80.97

Insert Which Layer: As the encoders in CLIP consist of multiple layers, the effect of inserting SEP into different layers is analyzed and summarized in Table 9. The best results were achieved by inserting the prompts into all layers.

Table 9: Effect of inserting SEP into different layers.

Layers	{4}	{8}	{10}	{4,8}	{4,8,10}	{3,6,9}	{2,4,6,8,10}	{1,2,3,4,5,6,7,8,9,10,11}
Base	84.66	84.62	85.16	85.38	85.44	85.32	86.27	85.98
New	74.8	76.07	75.34	75.19	75.41	74.95	75.92	76.49
H	79.43	80.12	79.95	79.96	80.11	79.80	80.76	80.96

Effect of Template Initialization In the proposed SEP, we initialized the templates with ‘X X X X { }’. We thus make a comparison with the hand-crafted templates, such as ‘a photo of { }’, ‘this is a photo { }’, and summarize the related results in Table 10. It can be observed that the proposed methods is less sensitive to the initialization of the template for the textual prompt tuning. The reason is that the self-enhanced prompt is major affected by the pre-trained tokens, having less relation to the template.

Table 10: Effect of Template Initialization

Templates	Base	New	H
‘a photo of a{ }’	85.58	75.89	80.44
‘this is a photo { }’	85.53	75.92	80.44
‘X X X X { }’	85.56	75.90	80.44

Effect of Prompt length In this section, we analyze the effect of prompt length for the Self-Enhanced Prompt tuning, *e.g.*, L_v and L_t for the visual and textual prompt tuning, respectively. As shown in Table 11, we can observe that the proposed SEP is less sensitive to the prompt length. For example, for setting SEP with the same L_t for textual prompt tuning, different methods obtain similar performance, which is also the same for the prompt length for the visual prompt.

Table 11: Effect of Prompt Length for L_t and L_v .

L_t	2	2	2	2	4	4	4	4	6	6	6	6	8	8	8	8	16	16	16	16
L_v	2	4	6	8	2	4	6	8	2	4	6	8	2	4	6	8	2	4	6	8
Base	85.38	85.43	85.45	85.56	85.56	85.56	85.62	85.51	85.87	85.98	85.88	85.85	85.91	85.92	85.93	85.88	85.99	85.94	85.94	85.91
New	76.27	75.91	75.99	75.82	75.82	75.90	75.82	75.94	76.22	76.49	75.98	75.92	75.48	75.92	75.89	75.84	76.35	76.02	76.03	76.24
H	80.57	80.38	80.44	80.40	80.40	80.44	80.42	80.44	80.76	80.96	80.63	80.58	80.36	80.61	80.60	80.55	80.88	80.68	80.68	80.79

5 Conclusion

To overcome the shortcoming that existing CoOp-based methods have the limited ability to capture the input-aware specific knowledge, we propose a novel Self-Enhanced Prompt tuning by utilizing the Token Fusion Module(TFM) to inject the discriminative knowledge contained in self-pretrained tokens into the self-enhanced prompts. Evaluation of several tasks and benchmarks verify the effectiveness of the proposed SEP for prompt tuning. In the proposed SEP, the choice of representative tokens is still an open and critical problem to improve the robustness and flexibility of the SEP.

References

- [1] Lorenzo Agnolucci, Alberto Baldrati, Francesco Todino, Federico Becattini, Marco Bertini, and Alberto Del Bimbo. Eco: Ensembling context optimization for vision-language models. In *Proceedings of the IEEE/CVF International Conference on Computer Vision*, pages 2811–2815, 2023.
- [2] Jean-Baptiste Alayrac, Jeff Donahue, Pauline Luc, Antoine Miech, Iain Barr, Yana Hasson, Karel Lenc, Arthur Mensch, Katherine Millican, Malcolm Reynolds, et al. Flamingo: a visual language model for few-shot learning. *Advances in Neural Information Processing Systems*, 35: 23716–23736, 2022.

- [3] Lukas Bossard, Matthieu Guillaumin, and Luc Van Gool. Food-101 - mining discriminative components with random forests. In David J. Fleet, Tomás Pajdla, Bernt Schiele, and Tinne Tuytelaars, editors, *Computer Vision - ECCV 2014 - 13th European Conference, Zurich, Switzerland, September 6-12, 2014, Proceedings, Part VI*, volume 8694 of *Lecture Notes in Computer Science*, pages 446–461. Springer, 2014. doi: 10.1007/978-3-319-10599-4_29. URL https://doi.org/10.1007/978-3-319-10599-4_29.
- [4] Guangyi Chen, Weiran Yao, Xiangchen Song, Xinyue Li, Yongming Rao, and Kun Zhang. PLOT: prompt learning with optimal transport for vision-language models. In *The Eleventh International Conference on Learning Representations, ICLR 2023, Kigali, Rwanda, May 1-5, 2023*. OpenReview.net, 2023. URL <https://openreview.net/pdf?id=zqwyBoXYnh>.
- [5] Eulrang Cho, Jooyeon Kim, and Hyunwoo J Kim. Distribution-aware prompt tuning for vision-language models. In *Proceedings of the IEEE/CVF International Conference on Computer Vision*, pages 22004–22013, 2023.
- [6] Mircea Cimpoi, Subhransu Maji, Iasonas Kokkinos, Sammy Mohamed, and Andrea Vedaldi. Describing textures in the wild. In *2014 IEEE Conference on Computer Vision and Pattern Recognition, CVPR 2014, Columbus, OH, USA, June 23-28, 2014*, pages 3606–3613. IEEE Computer Society, 2014. doi: 10.1109/CVPR.2014.461. URL <https://doi.org/10.1109/CVPR.2014.461>.
- [7] Jia Deng, Wei Dong, Richard Socher, Li-Jia Li, Kai Li, and Li Fei-Fei. Imagenet: A large-scale hierarchical image database. In *2009 IEEE Computer Society Conference on Computer Vision and Pattern Recognition (CVPR 2009), 20-25 June 2009, Miami, Florida, USA*, pages 248–255. IEEE Computer Society, 2009.
- [8] Alexey Dosovitskiy, Lucas Beyer, Alexander Kolesnikov, Dirk Weissenborn, Xiaohua Zhai, Thomas Unterthiner, Mostafa Dehghani, Matthias Minderer, Georg Heigold, Sylvain Gelly, Jakob Uszkoreit, and Neil Houlsby. An image is worth 16x16 words: Transformers for image recognition at scale. In *9th International Conference on Learning Representations, ICLR 2021, Virtual Event, Austria, May 3-7, 2021*. OpenReview.net, 2021. URL <https://openreview.net/forum?id=YicbFdNTTy>.
- [9] Li Fei-Fei, Robert Fergus, and Pietro Perona. Learning generative visual models from few training examples: An incremental bayesian approach tested on 101 object categories. *Comput. Vis. Image Underst.*, 106(1):59–70, 2007. doi: 10.1016/j.cviu.2005.09.012. URL <https://doi.org/10.1016/j.cviu.2005.09.012>.
- [10] Zhe Gan, Linjie Li, Chunyuan Li, Lijuan Wang, Zicheng Liu, Jianfeng Gao, et al. Vision-language pre-training: Basics, recent advances, and future trends. *Foundations and Trends® in Computer Graphics and Vision*, 14(3–4):163–352, 2022.
- [11] Haoran Gao, Hua Zhang, Xingguo Yang, Wenmin Li, Fei Gao, and Qiaoyan Wen. Generating natural adversarial examples with universal perturbations for text classification. *Neurocomputing*, 471:175–182, 2022. doi: 10.1016/j.neucom.2021.10.089. URL <https://doi.org/10.1016/j.neucom.2021.10.089>.
- [12] Peng Gao, Shijie Geng, Renrui Zhang, Teli Ma, Rongyao Fang, Yongfeng Zhang, Hongsheng Li, and Yu Qiao. Clip-adapter: Better vision-language models with feature adapters. *CoRR*, abs/2110.04544, 2021. URL <https://arxiv.org/abs/2110.04544>.
- [13] Kaiming He, Xinlei Chen, Saining Xie, Yanghao Li, Piotr Dollár, and Ross B. Girshick. Masked autoencoders are scalable vision learners. In *IEEE/CVF Conference on Computer Vision and Pattern Recognition, CVPR 2022, New Orleans, LA, USA, June 18-24, 2022*, pages 15979–15988. IEEE, 2022. doi: 10.1109/CVPR52688.2022.01553. URL <https://doi.org/10.1109/CVPR52688.2022.01553>.
- [14] Patrick Helber, Benjamin Bischke, Andreas Dengel, and Damian Borth. Eurosat: A novel dataset and deep learning benchmark for land use and land cover classification. *IEEE J. Sel. Top. Appl. Earth Obs. Remote. Sens.*, 12(7):2217–2226, 2019. doi: 10.1109/JSTARS.2019.2918242. URL <https://doi.org/10.1109/JSTARS.2019.2918242>.

- [15] Dan Hendrycks, Steven Basart, Norman Mu, Saurav Kadavath, Frank Wang, Evan Dorundo, Rahul Desai, Tyler Zhu, Samyak Parajuli, Mike Guo, Dawn Song, Jacob Steinhardt, and Justin Gilmer. The many faces of robustness: A critical analysis of out-of-distribution generalization. In *2021 IEEE/CVF International Conference on Computer Vision, ICCV 2021, Montreal, QC, Canada, October 10-17, 2021*, pages 8320–8329. IEEE, 2021. doi: 10.1109/ICCV48922.2021.00823. URL <https://doi.org/10.1109/ICCV48922.2021.00823>.
- [16] Chao Jia, Yinfei Yang, Ye Xia, Yi-Ting Chen, Zarana Parekh, Hieu Pham, Quoc V. Le, Yun-Hsuan Sung, Zhen Li, and Tom Duerig. Scaling up visual and vision-language representation learning with noisy text supervision. In Marina Meila and Tong Zhang, editors, *Proceedings of the 38th International Conference on Machine Learning, ICML 2021, 18-24 July 2021, Virtual Event*, volume 139 of *Proceedings of Machine Learning Research*, pages 4904–4916. PMLR, 2021.
- [17] Baoshuo Kan, Teng Wang, Wenpeng Lu, Xiantong Zhen, Weili Guan, and Feng Zheng. Knowledge-aware prompt tuning for generalizable vision-language models. In *Proceedings of the IEEE/CVF International Conference on Computer Vision*, pages 15670–15680, 2023.
- [18] Muhammad Uzair Khattak, Hanoona Rasheed, Muhammad Maaz, Salman Khan, and Fahad Shahbaz Khan. Maple: Multi-modal prompt learning. In *Proceedings of the IEEE/CVF Conference on Computer Vision and Pattern Recognition*, pages 19113–19122, 2023.
- [19] Muhammad Uzair Khattak, Syed Talal Wasim, Muzammal Naseer, Salman Khan, Ming-Hsuan Yang, and Fahad Shahbaz Khan. Self-regulating prompts: Foundational model adaptation without forgetting. In *Proceedings of the IEEE/CVF International Conference on Computer Vision*, pages 15190–15200, 2023.
- [20] Wonjae Kim, Bokyoung Son, and Ildoo Kim. Vilt: Vision-and-language transformer without convolution or region supervision. In Marina Meila and Tong Zhang, editors, *Proceedings of the 38th International Conference on Machine Learning, ICML 2021, 18-24 July 2021, Virtual Event*, volume 139 of *Proceedings of Machine Learning Research*, pages 5583–5594. PMLR, 2021. URL <http://proceedings.mlr.press/v139/kim21k.html>.
- [21] Jonathan Krause, Michael Stark, Jia Deng, and Li Fei-Fei. 3d object representations for fine-grained categorization. In *2013 IEEE International Conference on Computer Vision Workshops, ICCV Workshops 2013, Sydney, Australia, December 1-8, 2013*, pages 554–561. IEEE Computer Society, 2013. doi: 10.1109/ICCVW.2013.77. URL <https://doi.org/10.1109/ICCVW.2013.77>.
- [22] Dongjun Lee, Seokwon Song, Jihee Suh, Joonmyeong Choi, Sanghyeok Lee, and Hyunwoo J Kim. Read-only prompt optimization for vision-language few-shot learning. In *Proceedings of the IEEE/CVF International Conference on Computer Vision*, pages 1401–1411, 2023.
- [23] Juncheng Li, Minghe Gao, Longhui Wei, Siliang Tang, Wenqiao Zhang, Mengze Li, Wei Ji, Qi Tian, Tat-Seng Chua, and Yueting Zhuang. Gradient-regulated meta-prompt learning for generalizable vision-language models. *arXiv preprint arXiv:2303.06571*, 2023.
- [24] Junnan Li, Dongxu Li, Caiming Xiong, and Steven Hoi. Blip: Bootstrapping language-image pre-training for unified vision-language understanding and generation. In *International Conference on Machine Learning*, pages 12888–12900. PMLR, 2022.
- [25] Junnan Li, Dongxu Li, Silvio Savarese, and Steven Hoi. Blip-2: Bootstrapping language-image pre-training with frozen image encoders and large language models. *arXiv preprint arXiv:2301.12597*, 2023.
- [26] Xin Li, Dongze Lian, Zhihe Lu, Jiawang Bai, Zhibo Chen, and Xinchao Wang. Graphadapter: Tuning vision-language models with dual knowledge graph. In Alice Oh, Tristan Naumann, Amir Globerson, Kate Saenko, Moritz Hardt, and Sergey Levine, editors, *Advances in Neural Information Processing Systems 36: Annual Conference on Neural Information Processing Systems 2023, NeurIPS 2023, New Orleans, LA, USA, December 10 - 16, 2023*, 2023. URL http://papers.nips.cc/paper_files/paper/2023/hash/2b25c39788e5cf11d3541de433ebf4c0-Abstract-Conference.html.

- [27] Jiasen Lu, Dhruv Batra, Devi Parikh, and Stefan Lee. Vilbert: Pretraining task-agnostic visiolinguistic representations for vision-and-language tasks. In Hanna M. Wallach, Hugo Larochelle, Alina Beygelzimer, Florence d’Alché-Buc, Emily B. Fox, and Roman Garnett, editors, *Advances in Neural Information Processing Systems 32: Annual Conference on Neural Information Processing Systems 2019, NeurIPS 2019, December 8-14, 2019, Vancouver, BC, Canada*, pages 13–23, 2019. URL <https://proceedings.neurips.cc/paper/2019/hash/c74d97b01eae257e44aa9d5bade97baf-Abstract.html>.
- [28] Yuning Lu, Jianzhuang Liu, Yonggang Zhang, Yajing Liu, and Xinmei Tian. Prompt distribution learning. In *IEEE/CVF Conference on Computer Vision and Pattern Recognition, CVPR 2022, New Orleans, LA, USA, June 18-24, 2022*, pages 5196–5205. IEEE, 2022. doi: 10.1109/CVPR52688.2022.00514. URL <https://doi.org/10.1109/CVPR52688.2022.00514>.
- [29] Subhansu Maji, Esa Rahtu, Juho Kannala, Matthew B. Blaschko, and Andrea Vedaldi. Fine-grained visual classification of aircraft. *CoRR*, abs/1306.5151, 2013. URL <http://arxiv.org/abs/1306.5151>.
- [30] Maria-Elena Nilsback and Andrew Zisserman. Automated flower classification over a large number of classes. In *Sixth Indian Conference on Computer Vision, Graphics & Image Processing, ICVGIP 2008, Bhubaneswar, India, 16-19 December 2008*, pages 722–729. IEEE Computer Society, 2008. doi: 10.1109/ICVGIP.2008.47. URL <https://doi.org/10.1109/ICVGIP.2008.47>.
- [31] Yassine Ouali, Adrian Bulat, Brais Martinez, and Georgios Tzimiropoulos. Black box few-shot adaptation for vision-language models. In *Proceedings of the IEEE/CVF International Conference on Computer Vision*, pages 15534–15546, 2023.
- [32] Omkar M. Parkhi, Andrea Vedaldi, Andrew Zisserman, and C. V. Jawahar. Cats and dogs. In *2012 IEEE Conference on Computer Vision and Pattern Recognition, Providence, RI, USA, June 16-21, 2012*, pages 3498–3505. IEEE Computer Society, 2012. doi: 10.1109/CVPR.2012.6248092. URL <https://doi.org/10.1109/CVPR.2012.6248092>.
- [33] Alec Radford, Jong Wook Kim, Chris Hallacy, Aditya Ramesh, Gabriel Goh, Sandhini Agarwal, Girish Sastry, Amanda Askell, Pamela Mishkin, Jack Clark, Gretchen Krueger, and Ilya Sutskever. Learning transferable visual models from natural language supervision. In Marina Meila and Tong Zhang, editors, *Proceedings of the 38th International Conference on Machine Learning, ICML 2021, 18-24 July 2021, Virtual Event*, volume 139 of *Proceedings of Machine Learning Research*, pages 8748–8763. PMLR, 2021.
- [34] Yongming Rao, Wenliang Zhao, Guangyi Chen, Yansong Tang, Zheng Zhu, Guan Huang, Jie Zhou, and Jiwen Lu. Denseclip: Language-guided dense prediction with context-aware prompting. In *IEEE/CVF Conference on Computer Vision and Pattern Recognition, CVPR 2022, New Orleans, LA, USA, June 18-24, 2022*, pages 18061–18070. IEEE, 2022. doi: 10.1109/CVPR52688.2022.01755. URL <https://doi.org/10.1109/CVPR52688.2022.01755>.
- [35] Benjamin Recht, Rebecca Roelofs, Ludwig Schmidt, and Vaishal Shankar. Do imagenet classifiers generalize to imagenet? In Kamalika Chaudhuri and Ruslan Salakhutdinov, editors, *Proceedings of the 36th International Conference on Machine Learning, ICML 2019, 9-15 June 2019, Long Beach, California, USA*, volume 97 of *Proceedings of Machine Learning Research*, pages 5389–5400. PMLR, 2019. URL <http://proceedings.mlr.press/v97/recht19a.html>.
- [36] Christoph Schuhmann, Richard Vencu, Romain Beaumont, Robert Kaczmarczyk, Clayton Mullis, Aarush Katta, Theo Coombes, Jenia Jitsev, and Aran Komatsuzaki. Laion-400m: Open dataset of clip-filtered 400 million image-text pairs. *arXiv preprint arXiv:2111.02114*, 2021.
- [37] Christoph Schuhmann, Romain Beaumont, Richard Vencu, Cade Gordon, Ross Wightman, Mehdi Cherti, Theo Coombes, Aarush Katta, Clayton Mullis, Mitchell Wortsman, et al. Laion-5b: An open large-scale dataset for training next generation image-text models. *Advances in Neural Information Processing Systems*, 35:25278–25294, 2022.

- [38] Sheng Shen, Shijia Yang, Tianjun Zhang, Bohan Zhai, Joseph E. Gonzalez, Kurt Keutzer, and Trevor Darrell. Multitask vision-language prompt tuning. *CoRR*, abs/2211.11720, 2022. doi: 10.48550/ARXIV.2211.11720. URL <https://doi.org/10.48550/arXiv.2211.11720>.
- [39] Amanpreet Singh, Ronghang Hu, Vedanuj Goswami, Guillaume Couairon, Wojciech Galuba, Marcus Rohrbach, and Douwe Kiela. Flava: A foundational language and vision alignment model. In *Proceedings of the IEEE/CVF Conference on Computer Vision and Pattern Recognition*, pages 15638–15650, 2022.
- [40] Khurram Soomro, Amir Roshan Zamir, and Mubarak Shah. UCF101: A dataset of 101 human actions classes from videos in the wild. *CoRR*, abs/1212.0402, 2012. URL <http://arxiv.org/abs/1212.0402>.
- [41] Jingchen Sun, Jiayu Qin, Zihao Lin, and Changyou Chen. Prompt tuning based adapter for vision-language model adaption. *CoRR*, abs/2303.15234, 2023. doi: 10.48550/ARXIV.2303.15234. URL <https://doi.org/10.48550/arXiv.2303.15234>.
- [42] Ashish Vaswani, Noam Shazeer, Niki Parmar, Jakob Uszkoreit, Llion Jones, Aidan N. Gomez, Lukasz Kaiser, and Illia Polosukhin. Attention is all you need. In Isabelle Guyon, Ulrike von Luxburg, Samy Bengio, Hanna M. Wallach, Rob Fergus, S. V. N. Vishwanathan, and Roman Garnett, editors, *Advances in Neural Information Processing Systems 30: Annual Conference on Neural Information Processing Systems 2017, December 4-9, 2017, Long Beach, CA, USA*, pages 5998–6008, 2017. URL <https://proceedings.neurips.cc/paper/2017/hash/3f5ee243547dee91fbd053c1c4a845aa-Abstract.html>.
- [43] Haohan Wang, Songwei Ge, Zachary C. Lipton, and Eric P. Xing. Learning robust global representations by penalizing local predictive power. In Hanna M. Wallach, Hugo Larochelle, Alina Beygelzimer, Florence d’Alché-Buc, Emily B. Fox, and Roman Garnett, editors, *Advances in Neural Information Processing Systems 32: Annual Conference on Neural Information Processing Systems 2019, NeurIPS 2019, December 8-14, 2019, Vancouver, BC, Canada*, pages 10506–10518, 2019. URL <https://proceedings.neurips.cc/paper/2019/hash/3eefceb8087e964f89c2d59e8a249915-Abstract.html>.
- [44] Jianxiong Xiao, James Hays, Krista A. Ehinger, Aude Oliva, and Antonio Torralba. SUN database: Large-scale scene recognition from abbey to zoo. In *The Twenty-Third IEEE Conference on Computer Vision and Pattern Recognition, CVPR 2010, San Francisco, CA, USA, 13-18 June 2010*, pages 3485–3492. IEEE Computer Society, 2010. doi: 10.1109/CVPR.2010.5539970. URL <https://doi.org/10.1109/CVPR.2010.5539970>.
- [45] Hantao Yao, Rui Zhang, and Changsheng Xu. Visual-language prompt tuning with knowledge-guided context optimization. In *Proceedings of the IEEE/CVF Conference on Computer Vision and Pattern Recognition*, pages 6757–6767, 2023.
- [46] Hantao Yao, Rui Zhang, and Changsheng Xu. Tcp: Textual-based class-aware prompt tuning for visual-language model. In *CVPR*, 2024.
- [47] Tao Yu, Zhihe Lu, Xin Jin, Zhibo Chen, and Xinchao Wang. Task residual for tuning vision-language models. In *IEEE/CVF Conference on Computer Vision and Pattern Recognition, CVPR 2023, Vancouver, BC, Canada, June 17-24, 2023*, pages 10899–10909. IEEE, 2023. doi: 10.1109/CVPR52729.2023.01049. URL <https://doi.org/10.1109/CVPR52729.2023.01049>.
- [48] Yuhang Zang, Wei Li, Kaiyang Zhou, Chen Huang, and Chen Change Loy. Unified vision and language prompt learning. *CoRR*, abs/2210.07225, 2022. doi: 10.48550/arXiv.2210.07225. URL <https://doi.org/10.48550/arXiv.2210.07225>.
- [49] Xiaohua Zhai, Alexander Kolesnikov, Neil Houlsby, and Lucas Beyer. Scaling vision transformers. In *Proceedings of the IEEE/CVF Conference on Computer Vision and Pattern Recognition*, pages 12104–12113, 2022.
- [50] Ji Zhang, Shihan Wu, Lianli Gao, Hengtao Shen, and Jingkuan Song. Dept: Decoupled prompt tuning. In *CVPR*, 2024.

- [51] Kaiyang Zhou, Jingkang Yang, Chen Change Loy, and Ziwei Liu. Conditional prompt learning for vision-language models. In *IEEE/CVF Conference on Computer Vision and Pattern Recognition, CVPR 2022, New Orleans, LA, USA, June 18-24, 2022*, pages 16795–16804. IEEE, 2022. doi: 10.1109/CVPR52688.2022.01631. URL <https://doi.org/10.1109/CVPR52688.2022.01631>.
- [52] Kaiyang Zhou, Jingkang Yang, Chen Change Loy, and Ziwei Liu. Learning to prompt for vision-language models. *Int. J. Comput. Vis.*, 130(9):2337–2348, 2022. doi: 10.1007/s11263-022-01653-1. URL <https://doi.org/10.1007/s11263-022-01653-1>.
- [53] Beier Zhu, Yulei Niu, Yucheng Han, Yue Wu, and Hanwang Zhang. Prompt-aligned gradient for prompt tuning. In *Proceedings of the IEEE/CVF International Conference on Computer Vision*, pages 15659–15669, 2023.
- [54] Beier Zhu, Yulei Niu, Saeil Lee, Minhoe Hur, and Hanwang Zhang. Debaised fine-tuning for vision-language models by prompt regularization. In Brian Williams, Yiling Chen, and Jennifer Neville, editors, *Thirty-Seventh AAAI Conference on Artificial Intelligence, AAAI 2023, Thirty-Fifth Conference on Innovative Applications of Artificial Intelligence, IAAI 2023, Thirteenth Symposium on Educational Advances in Artificial Intelligence, EAAI 2023, Washington, DC, USA, February 7-14, 2023*, pages 3834–3842. AAAI Press, 2023. doi: 10.1609/AAAI.V37I3.25496. URL <https://doi.org/10.1609/aaai.v37i3.25496>.